Electronic Supplementary Material (ESI) for Journal of Materials Chemistry A.
This journal is © The Royal Society of Chemistry 2024

Supporting Information

for

Cation exchange improves the efficiency and stability of the n-doping of π-conjugated polymers

Jingyu Li [a], *Sihui Deng* [b, c], *Junli Hu* [a, *], *Yichun Liu* [a]

a Key Laboratory of UV-Emitting Materials and Technology, Northeast Normal University, Ministry of Education, Changchun, Jilin, 130024, China

b State Key Laboratory of Polymer Physics and Chemistry, Changchun Institute of Applied Chemistry, Chinese Academy of Sciences, Changchun, Jilin, 130022, China

c University of Science and Technology of China, Hefei, Anhui, 230026, China

* Corresponding author at hujl100@nenu.edu.cn.

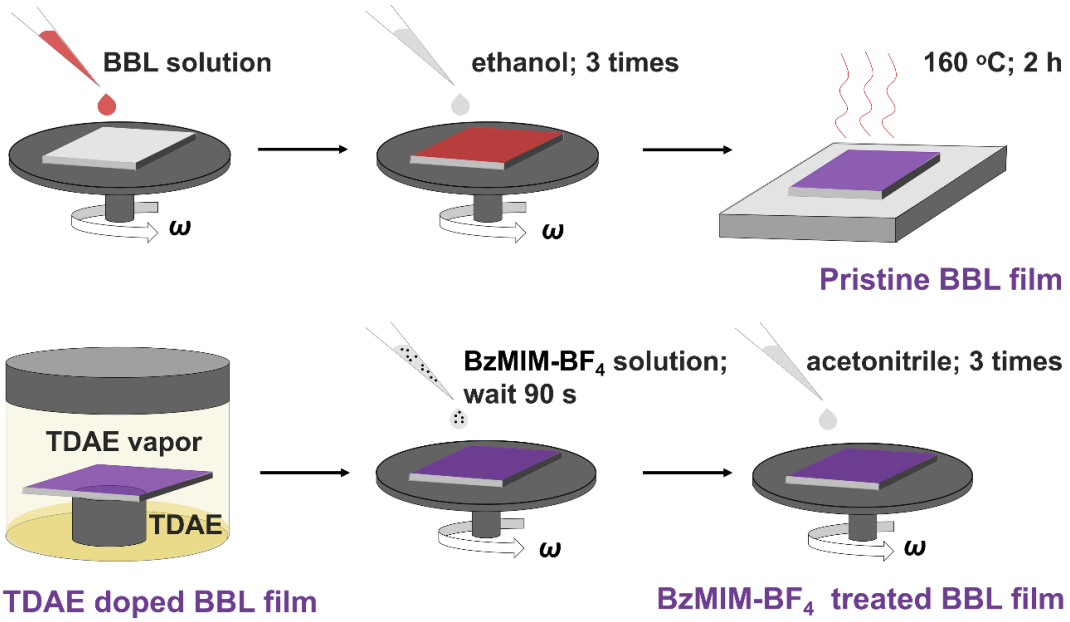

Figure S1. Schematic illustration of the processes of device fabrication.

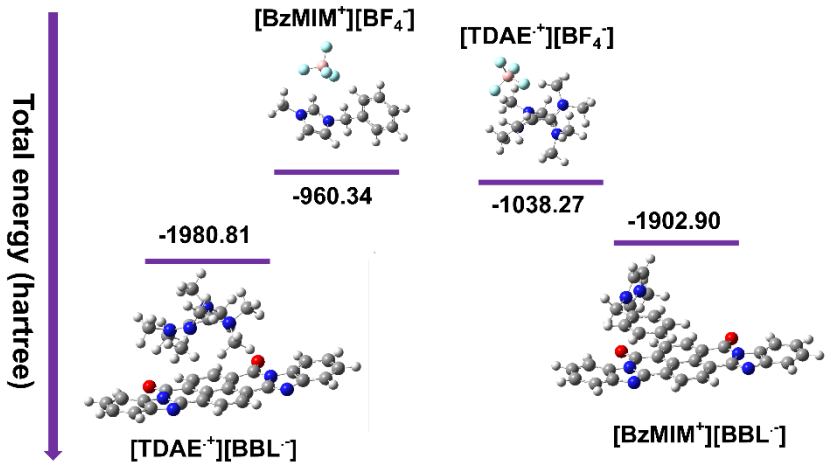

Figure S2. The optimized structures and total energy of different ion pairs. The total energy values for ion pairs as calculated using the B3LYP functional and the def2-SVP basis set.

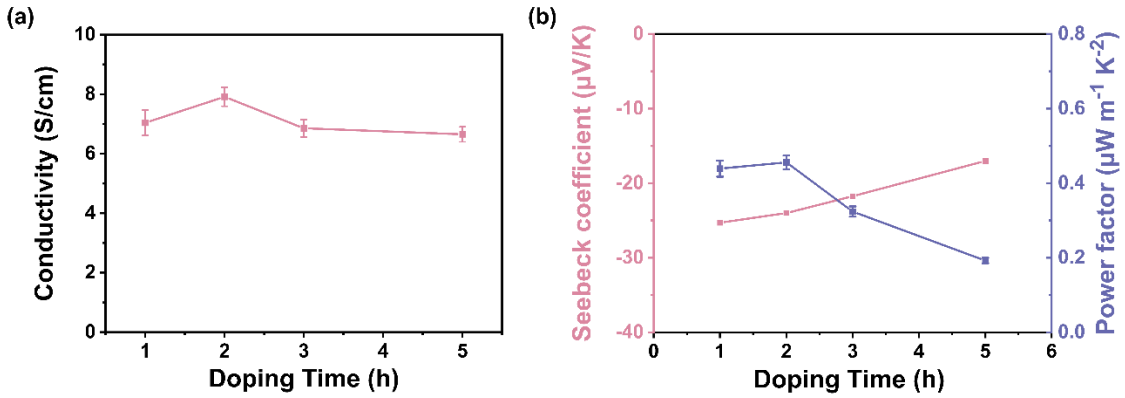

Figure S3. The effect of doping time of TDAE on (a) the conductivity and (b) the thermoelectric performance of the BBL film.

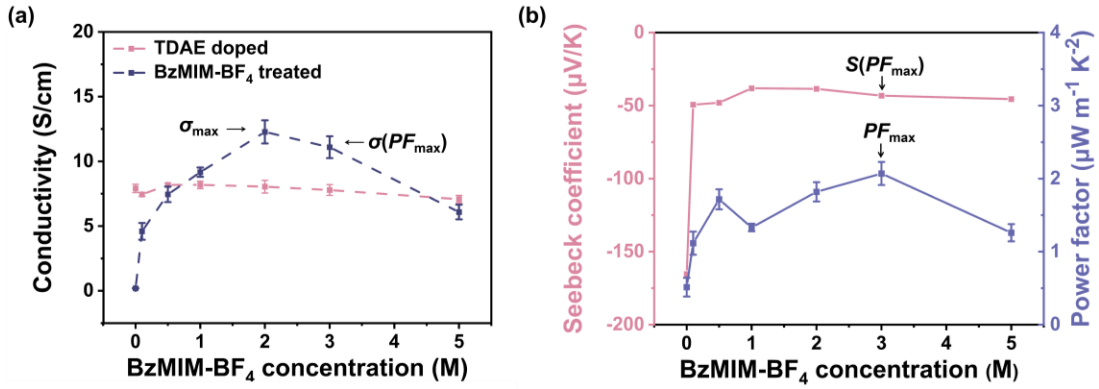

Figure S4. (a) Conductivity and (b) thermoelectric performance of the BBL films treated with BzMIM-BF_4 solution of different concentrations. The concentration of 0 M implies pure acetonitrile treatment.

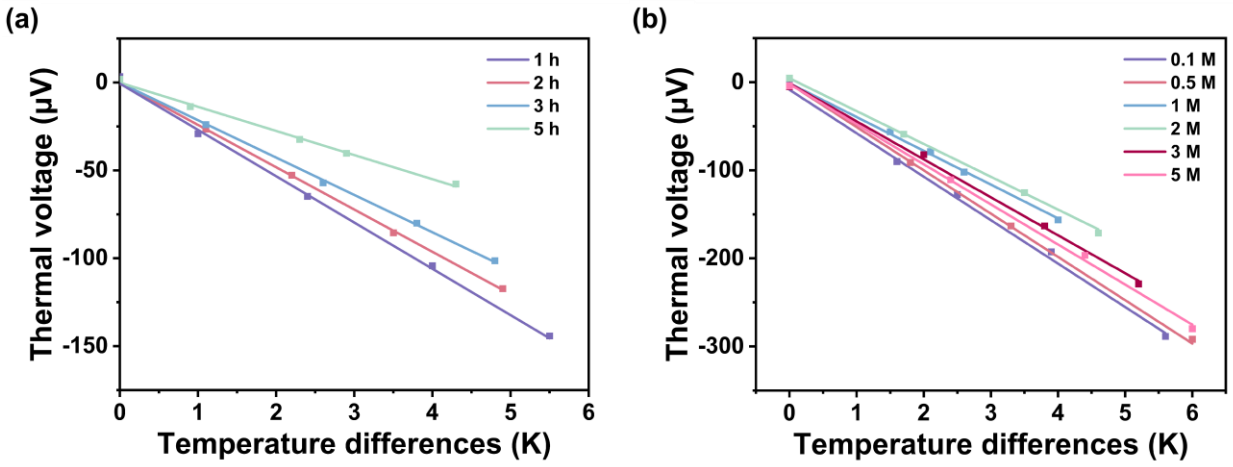

Figure S5. Temperature difference dependent thermal voltage of a) TDAE doped BBL films at different doping times and b) BzMIM-BF_4 treated BBL films at different concentrations.

Table S1. Summary of conductivity of BBL films reported in literatures.

Polymer: dopant	Doping method	σ_{max} (S/cm)	Ref
BBL: TDAE: BzMIM-BF_4	Cation exchange	12.3	This work
BBL: N-DMBI	Sequential doping	4.4	32
	Sequential doping	11.0	47
BBL: PEI	Blending doping	8.0	40
BBL: $BV^{\bullet+}$	Sequential doping	1.6	44
BBL: P(g42T-T)	Blending doping	0.2	42
BBL: TDAE	Vapor doping	1.7	39

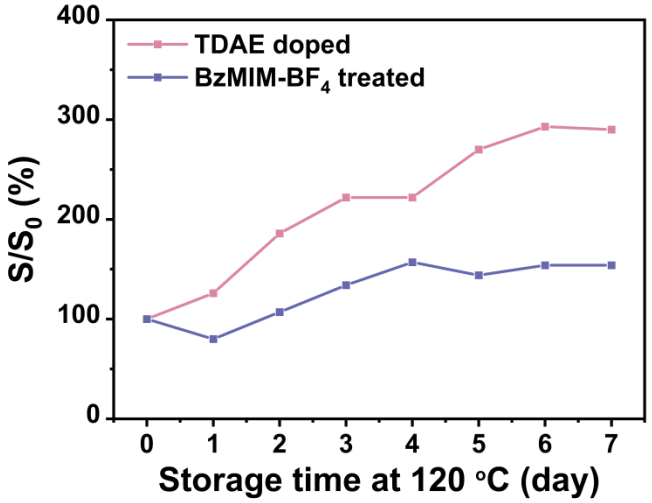

Figure S6. The change of the normalized Seebeck coefficient of the TDAE doped and BzMIM-BF_4 treated BBL films during the storage at 120 °C under nitrogen atmosphere.

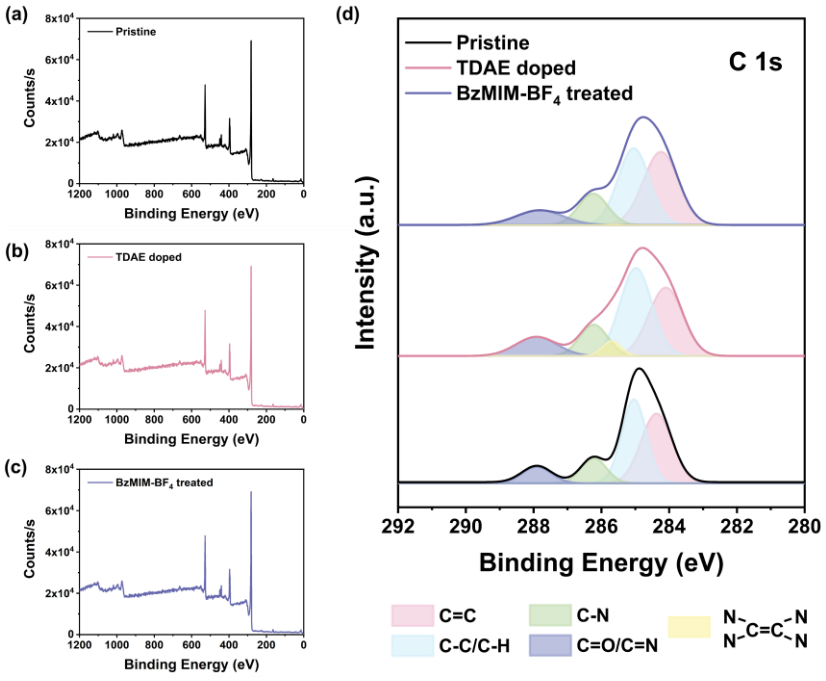

Figure S7. The XPS spectra of the (a) pristine, (b)TDAE doped and (c) BzMIM-BF_4 treated BBL films. (d)The XPS spectra analysis of C 1s for the pristine, TDAE doped and BzMIM-BF_4 treated BBL films.

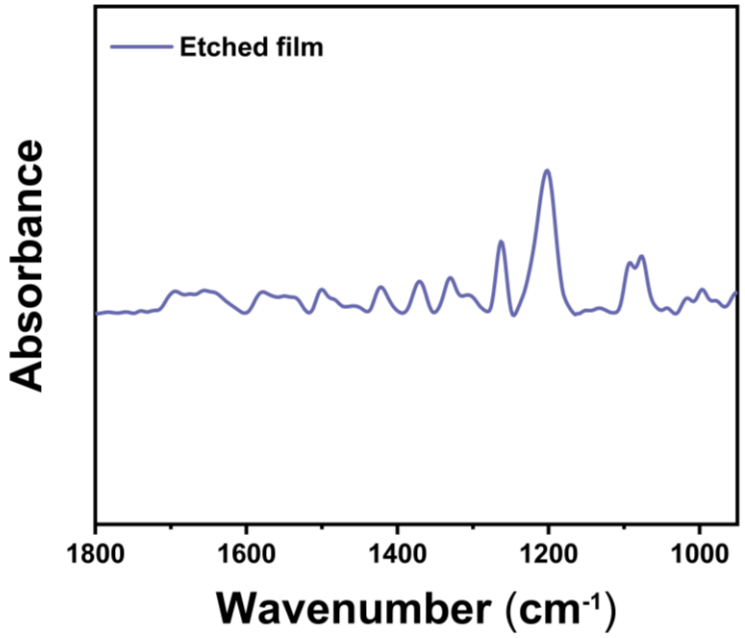

Figure S8. The FTIR spectra of BzMIM-BF_4 treated BBL film etched by nitrogen plasma. The thickness of the etched film was 28 nm.

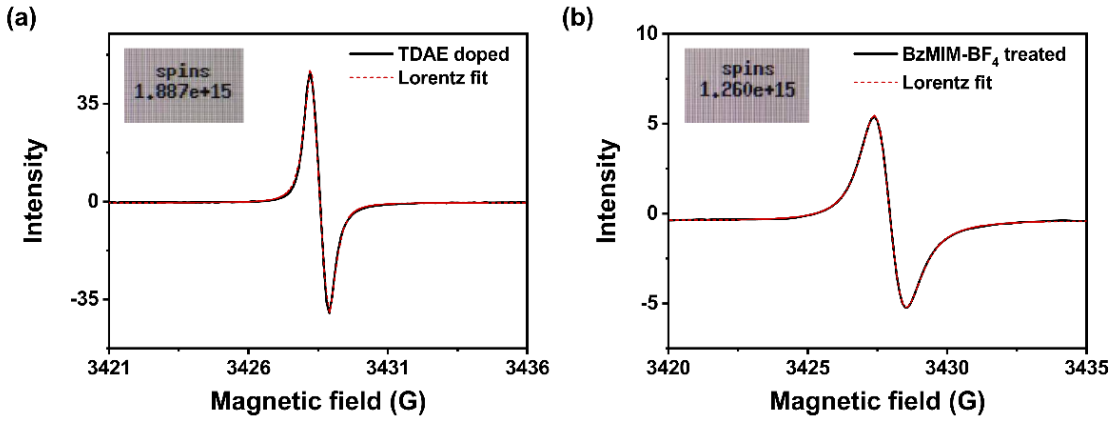

Figure S9. The spins calculation and the Lorentz fit of EPR curves of (a) the TDAE doped and (b) the BzMIM-BF_4 treated BBL films.

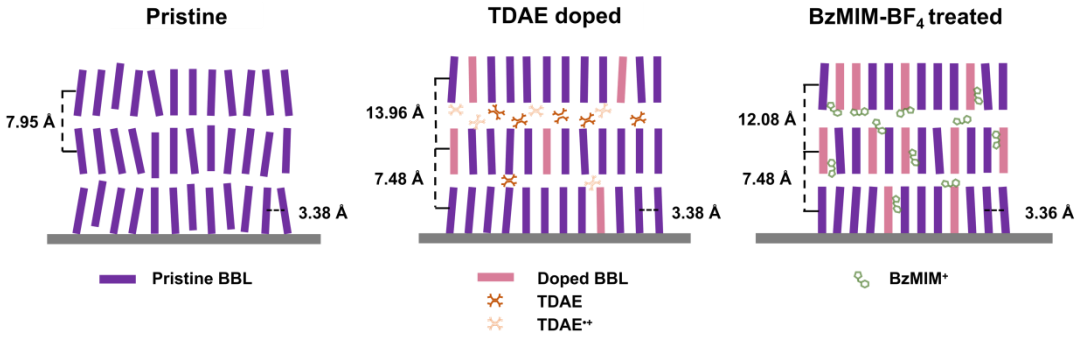

Figure S10. Schematic illustration of the microstructure of the BBL films.

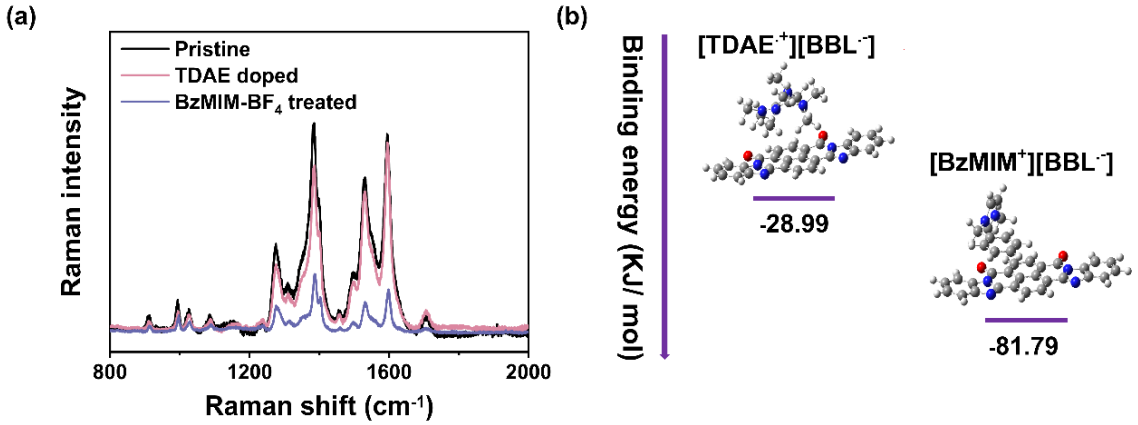

Figure S11. (a) The Raman spectra of the BBL films. (b) The binding energy between different cations and polarons.

Table S2. The GIWAXS analysis of the pristine, TDAE doped and BzMIM-BF_4 treated BBL films. Coherence length, and paracrystallinity in in-plane (010) diffraction.

Sample	Coherence length (Å)	Paracrystallinity (%)
Pristine BBL film	35.12	3.43
TDAE doped BBL film	44.87	3.04
BzMIM-BF_4 treated BBL film	43.83	3.05